TOPICAL REVIEW

Visualizing biological reaction intermediates with DNA curtains

To cite this article: Yiling Zhao *et al* 2017 *J. Phys. D: Appl. Phys.* **50** 153001

IOP Publishing Journal of Physics D: Applied Physics

J. Phys. D: Appl. Phys. **50** (2017) 153001 (16pp) https://doi.org/10.1088/1361-6463/aa59cf

Topical Review

Visualizing biological reaction intermediates with DNA curtains

Yiling Zhao[1,2], Yanzhou Jiang[1,2] and Zhi Qi[1,2]

[1] Center for Quantitative Biology, Academy for Advanced Interdisciplinary Studies, Peking University, Beijing 100871, People's Republic of China
[2] Peking-Tsinghua Center for Life Sciences, Academy for Advanced Interdisciplinary Studies, Peking University, Beijing 100871, People's Republic of China

E-mail: zhiqi7@pku.edu.cn

Received 26 April 2016, revised 8 January 2017
Accepted for publication 17 January 2017
Published 10 March 2017

Abstract

Single-molecule approaches have tremendous potential analyzing dynamic biological reaction with heterogeneity that cannot be effectively accessed via traditional ensemble-level biochemical approaches. The approach of deoxyribonucleic acid (DNA) curtains developed by Dr Eric Greene and his research team at Columbia University is a high-throughput single-molecule technique that utilizes fluorescent imaging to visualize protein–DNA interactions directly and allows the acquisition of statistically relevant information from hundreds or even thousands of individual reactions. This review aims to summarize the past, present, and future of DNA curtains, with an emphasis on its applications to solve important biological questions.

Keywords: single-molecule biophysics, total internal reflection fluorescence microscopy, double-stranded DNA (dsDNA), single-stranded DNA (ssDNA), DNA curtains, base pair

S Supplementary material for this article is available online

(Some figures may appear in colour only in the online journal)

1. Introduction

Tremendous progress in our understanding of DNA metabolism in cells has been made through multi-disciplinary research endeavors [1]. Emerging techniques, such as single-molecule approaches, start to reveal mechanistic details underlying DNA metabolic processes, e.g. DNA replication, transcription and DNA damage repair [2–8]. In contrast to traditional techniques based on ensemble averaging, single-molecule approaches directly visualize transient biochemical intermediates and heterogeneous reactions in unprecedented detail, hence, offer a bright prospect for filling in our knowledge of transient intermediate states during important biological reactions.

Single-molecule biophysics [9] can be roughly classified into two groups: (i) fluorescence related approaches, e.g. single-molecule fluorescence resonance energy transfer (smFRET) [10] and DNA curtains (figures 1 and 2) [11, 12]; and (ii) force related methods, e.g. optical tweezers, magnetic tweezers, and atomic force microscopy [13]. Compared with other single-molecule approaches, the DNA curtains method has its distinctive flavor. The first characteristic is high-throughput method. In contrast to the most single-molecule force related methods: one molecule at a time, DNA curtains use hundreds or even thousands of molecules at a time. However, 'high-throughput' is not unique only for the DNA curtains method, single-molecule fluorescence related approaches, like smFRET [10] and single-molecule pull down [14] are also high-throughput techniques. The second characteristic is long spatial range of DNA substrates. In contrast to smFRET or pull down methods in which only short DNA substrates can be used, the DNA curtains approach can use long spatial range of DNA molecules. So the DNA curtains method is the key solution for many biological questions. For example, (i) helicase displaces dsDNA binding proteins on

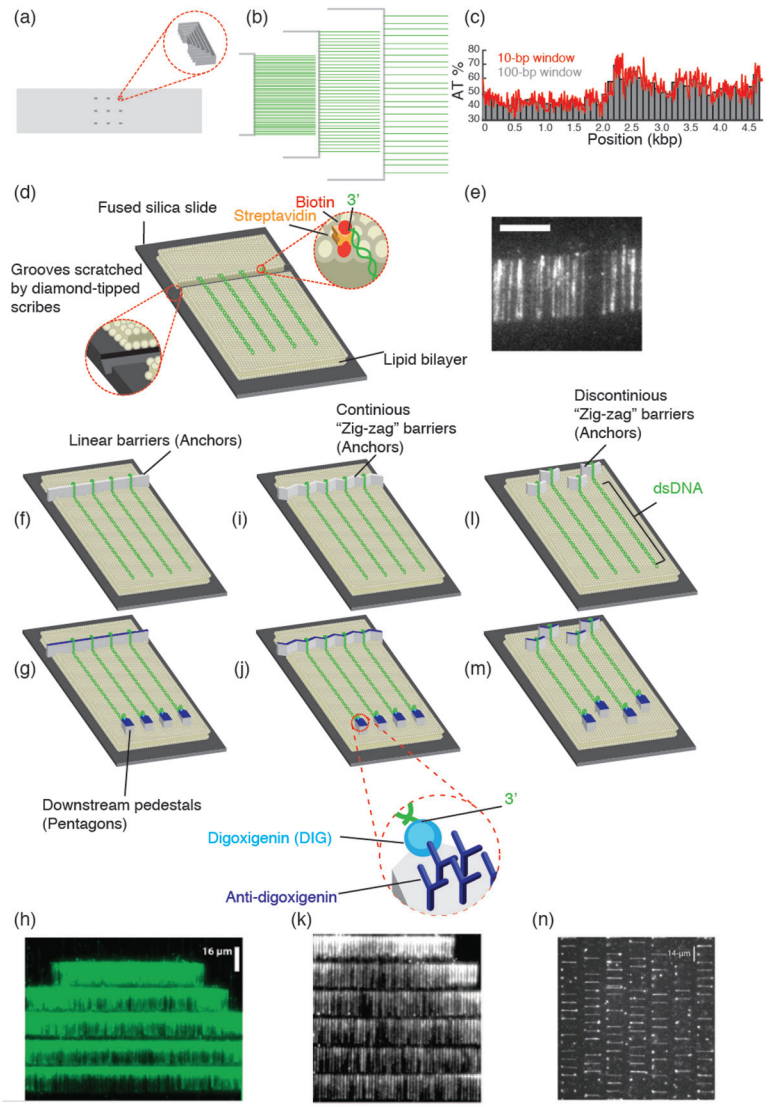

Figure 1. Schematic of a flowcell for dsDNA curtains. (a) Schematic of a quartz microscope slide with diffusion barriers. There is a 3 × 3 matrix, and each unit on the matrix is a set of diffusion barriers. DNA substrates will be injected from the left, and pushed to the right. (b) Schematic of single-tethered dsDNA curtains. One end of DNA substrates (green line) are tethered in front of the diffusion barriers, and are extended with flow. (c) AT% dependence of Lambda DNA, which is the DNA substrate for DNA curtains. (d) Schematic of flowcell with Barrier 1.0 [24, 25]. Insert represents biotin–streptavidin interaction, tethering one end of DNA molecules before the diffusion barriers. (e) TIRFM imaging of DNA curtains with Barrier 1.0. (f), (g), (i), (j), (l) and (m) Schematic of flowcell with Barrier 2.0 [27], 3.0 [26], and 4.0 [28]. Figures (e), (g) and (i) are for ST, and figures (f), (h) and (j) are for DT. (h), (k) and (n) TIRFM imaging of DNA curtains with Barrier 2.0, 3.0, and 4.0. Insert of (j) represents DIG–AntiDIG interaction, tethering the opposite ends of DNA molecules as they interact with the antibodies on the pentagons. Figure (c) is reprinted from [42], Copyright (2015), with permission from Elsevier. Figure (e) is reprinted with permission from [23]. Copyright (2006) American Chemical Society. Figure (h) is reprinted with permission from [26]. Copyright (2008) American Chemical Society. Figure (k) is reprinted with permission from [25]. Copyright (2008) American Chemical Society. Figure (n) is reprinted by permission from Macmillan Publishers Ltd: Nature Structural and Molecular Biology [27], copyright (2012).

long spatial range of dsDNA (sections 3.2 and 3.3) [15]; (ii) off-targets can be monitored directly when CRISPR associated protein 9–Ribonucleic acid (Cas9–RNA, and CRISPR is clustered regularly interspaced short palindromic repeats) complex searches on dsDNA (section 3.1.3) [16, 17]; (iii) MutSα and MutLα search lesion on dsDNA by intersite transfer during mismatch repair (section 3.1.1) [18]. The third characteristic is the sticking problem. The position of the diffusion barrier (section 2.1) can distinguish proteins on the DNA molecule from proteins stuck on the surface. However, smFRET or pull down methods are not easy to recognize in both cases.

This review focuses on the DNA curtains method [18–21], a powerful and flexible experimental platform firstly developed by Dr Eric Greene and his research team and capable of collecting statistically relevant information from hundreds or even thousands of individual reactions, allowing 'high-throughput' data analysis on DNA–protein interactions at the single-molecule level. Herein, following the chronological order, we review the development of double stranded DNA (dsDNA) and single stranded DNA (ssDNA) curtains (section 2), and their applications (sections 3 and 4) and conclude with a discussion of future prospects (section 5).

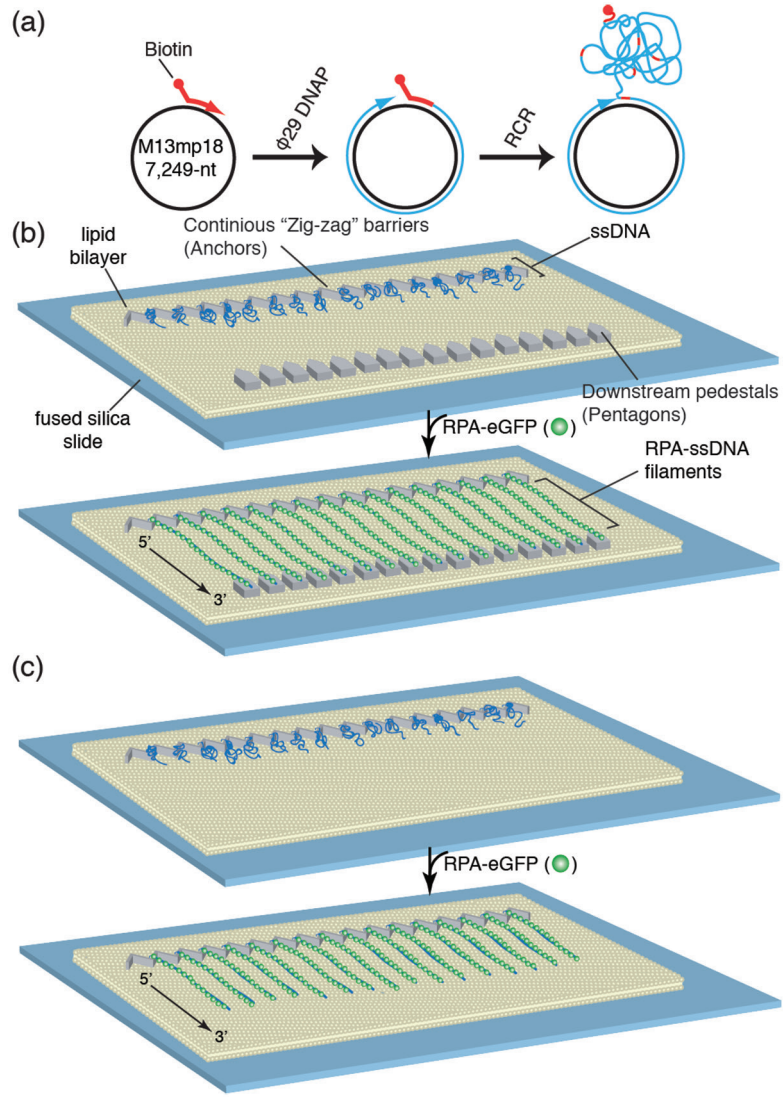

Figure 2. Schematic of ssDNA curtains. (a) Schematic of the rolling circle reaction. This reaction is used to prepare long ssDNA molecules for ssDNA curtains in (b) and (c). (b) Schematic of ssDNA curtains formation in a DT nanofabricated microfluidic flowcell. (c) Schematic of ssDNA curtains formation in a single-tethered nanofabricated microfluidic flowcell. RPA–eGFP is used to extend ssDNA molecules. Reprinted from [3], Copyright (2015), with permission from Elsevier.

2. The DNA curtains setup

Setting up the dsDNA (figure 1 and supplementary video 1 (stacks.iop.org/JPhysD/50/153001/mmedia)) and ssDNA (figure 2 and supplementary video 4) curtains has been elaborated upon in other reviews [11, 12, 22]. In brief, the surface of a microfluidic sample chamber is coated with a fluid lipid bilayer, and biotinylated DNA molecules are tethered to individual lipids within the bilayer through biotin–streptavidin interactions (insert in figure 1(d)). The bilayer renders the surface inert by shielding the sample material from the high uniform charge of the glass. The bilayer also mimics a cell membrane and is more 'natural' than other surfaces. The bilayer permits the movement of tethered DNA molecules in both dimensions while confining them near the flowcell surface. Hydrodynamic force is applied to align the DNA molecules along the leading edges of nanofabricated diffusion barriers, allowing the visualization of hundreds of individual DNAs in a field-of-view using total internal reflection fluorescence microscopy (TIRFM). The barriers are made by electron-beam lithography, and simple variations in barrier design allow precise control over the distribution and tethering geometry of the DNA molecules [23–28]. To understand the setup of DNA curtains in greater detail, we will elaborate the manipulation of three important components, viz. diffusion barriers, the microfluidic system, and DNA molecules.

2.1. Diffusion barriers

Preparing diffusion barriers (figure 1) on a fused silica slide is a key step of the DNA curtains approach. The lipid bilayer provides a 'bio-friendly' environment and the fluidic biomembranes allow rapid lateral movement of the lipids, causing tethered DNA substrates to diffuse. Diffusion barriers can block one end of each DNA molecule (attached to a lipid, insert in figure 1(d)), aligning them into arrays with patterns. The first generation of diffusion barriers (Barrier 1.0) was created in 2006 (figures 1(d) and (e)) [23, 24]. Afterwards Barrier 2.0

(figures 1(f) and (h)) [26], Barrier 3.0 (the current version, figures 1(i) and (k)) [25], and Barrier 4.0 (figures 1(l) and (n)) [27] were developed. Many reviews [11, 22, 24] have described the diffusion barrier designs very well, and here we just make a short summary and highlight the current version (Barrier 3.0).

Barrier 1.0 (figures 1(d) and (e)) [23, 24] is created on a quartz microscope slide. The quartz microscope slides were mechanically scratched with a diamond-tipped scribe to create ridges and grooves (imagine a 'V' shape cross section, but with the edges elevated), which are essentially the glass walls. Although this method successfully provides DNA curtains, mechanical etching cannot guarantee that all DNA molecules that are blocked by the same glass wall have the same initial tethering positions. For properly measuring position distributions, the nanofabrication techniques 'electron-beam lithography and thermal evaporation' are applied to produce Barrier 2.0 (figures 1(f) and (h)) [26], which is a chromium wall with a straight line shape, 30 nm high, and 100 nm width. The problem of initial positions is fixed, however, another question is found: DNA substrates diffuse laterally along the straight barriers, making the measurements difficult. To answer this question, Barrier 3.0 (figures 1(i) and (k)) [25] is designed to have a 'zig-zag' shape, restricting DNA substrates' lateral diffusions perfectly. Barrier 3.0 is the current version, and most of the DNA curtains experiments are performed on this kind of barrier design. To perform high-throughput double-tethered (DT) experiments, the downstream pedestals (pentagons) are added in conjunction with Barrier 2.0–4.0 (figures 1(g), (j) and (m)) [28]. Digoxigenin (DIG) on DNA molecule interacts anti-digoxigenin (antiDIG) on the surface of pentagons, tethering another end of DNA substrates (Insert in figure 1(j)). We note that Gorman *et al* [29] already generated DT molecules with Barrier 1.0, however, his method is not high-throughput.

A serious concern about Barrier 1.0–3.0 is that individual DNA substrate is difficult to be distinguished. Initial concentration of DNA substrates has to be tested on DNA curtains to determine an optimize experimental condition, which includes more cases with single DNA molecule per 'zig-zag' well. For this point, the continuous patterns can be changed to discontinuous patterns (Barrier 4.0, figure 1(l)), and the image of DNA curtains is shown in figure 1(n) [27].

2.2. Microfluidic system

The microfluidic system consists of syringe pumps, 6-port rotary valves (SCIVEX/RHEODYNE IDEX), DuPont PFA tubing (IDEX), and appropriate connecting ports (IDEX). The system is shown schematically in figure 3(a). As many as 'X number' different buffers can be loaded individually by syringes to pass a 4-port switching valve (IDEX)., which enables an easy switch among working buffers. Moreover, by switching a 6-port rotary valve between two positions referred to as 'Inject' and 'Load' modes (figure 3(a)), this microfluidic system can accurately transport a very small amount of biological samples into the flowcell to save sample. (i) in the 'Load' mode, the main microfluidic pathway is disconnected from the sample loop to allow the loading of biological samples. The sample loop is user-defined, and can accommodate almost any volume. 50 μl and 500 μl sample loops are diagrammed in figures 3(b) and (c); (ii) in 'Inject' mode, the main microfluidic pathway is connected with the sample loop, so the flow coming from the pump will push the sample buffer out of the loop. After a short delay, the biological sample will reach the flowcell and then the buffer flow is turned off to retain the sample in the flowcell. The accurate measurement of 'sample delay time' for a particular microfluidic system guarantees that samples are properly injected into a flowcell, and this is a key factor for successful DNA curtain experiments. The sample delay time depends on the total tubing length before entering the flowcell (figure 3(a)), the sample loop volume, the flow rate (figures 3(b) and (c)), and the response time of the syringe pump (figure 3(d)). The response time is defined as the waiting time for a syringe pump to reach the designated flow rate after it is turned on. It is important to note that the syringe pump retains a residual pressure on the system even after it is turned off: it takes time for the pressure to equilibrate. Therefore, a stopcock is recommended in-line with the pump to enable the stopping and starting of a flow in a sharply defined manner.

2.3. DNA molecules

The DNA molecules used in DNA curtains can be either dsDNA or ssDNA. (i) lambda DNA (48 502 bp) is often used as dsDNA substrate because of two main reasons: (a) lambda DNA is commercially available; (b) the sequence of lambda DNA shows a adenine-thymine (AT) content dependence (figure 1(c)): the first half region has a low AT%, and the second half with a relatively higher value of AT content. This property can be used to directly test whether a dsDNA binding protein depends on DNA sequence or not. Lambda DNA has two 12-nt 5′ overhangs (5′ – GGG CGG CGA CCT – 3′ and 5′ – AGG TCG CCG CCC – 3′), which are part of the cos site, and are called 'cos ends'. They are also called 'cohesive ends' albeit less prevalent, since other sequences can be 'cohesive'. A 12-nt oligo labeled with a biotin or a DIG at the 3′ end is designed to anneal and ligate to the 'cos end', forming the dsDNA substrates for ST or DT dsDNA curtains experiments; (ii) For ssDNA curtains, rolling circle reactions (RCRs) (figure 2(a)) are used to produce long ssDNA substrates [30]. A biotinylated oligo (5′ – BIOTIN – TTT TTT TTT TTT TTT TTT TTT TTT TTT TTT – GTA AAA CGA CGG CCA GT – 3′) is annealed to a M13 ssDNA circular template (M13mp18 from NEB) to form the RCR template, and then Φ29 DNA polymerase replicates multiple rounds on the RCR template in the presence of a deoxyribonucleotide (dNTP) mix (NEB) to produce a long ssDNA molecule.

3. Double-stranded DNA curtains

The dsDNA curtains method [18–21] form a novel and high-throughput experimental platform to study of protein–DNA interactions, by directly visualizing hundreds to thousands of individual binding reactions in real-time, thereby surmounting the one-experiment-one-data-point limit pervasive in single-molecule methods [31]. This section will focus on the biological applications of the dsDNA curtains method.

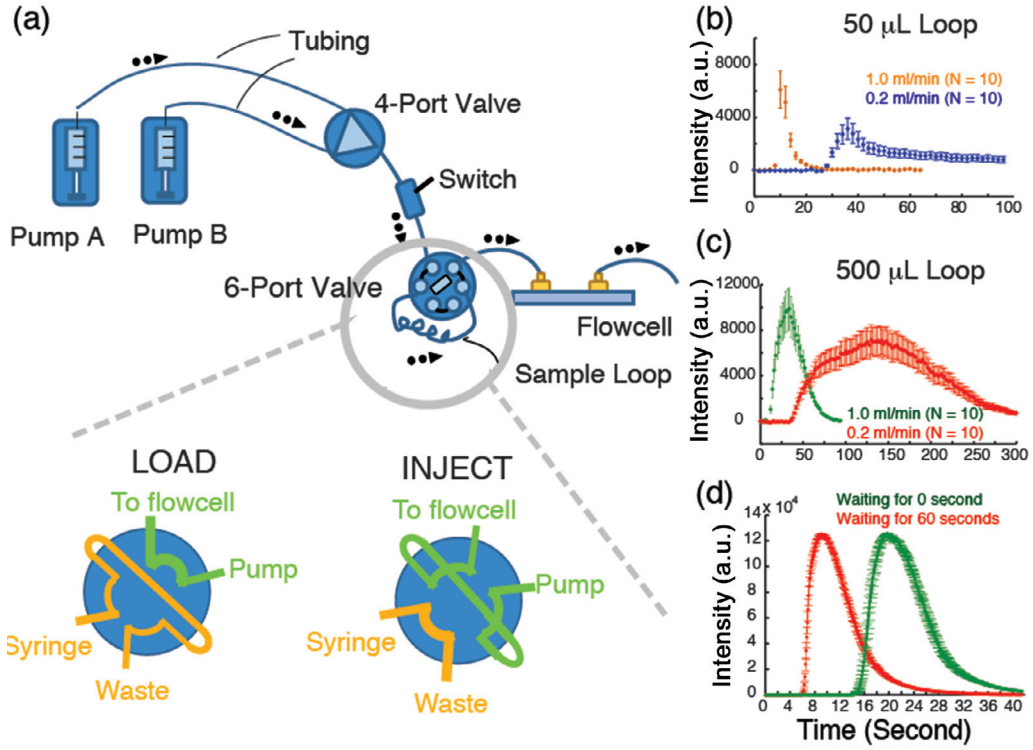

Figure 3. Microfluidic system. (a) Schematic of microfluidic system. (b) and (c) The measurement of the sample waiting time. (d) The influence of the response time of the syringe pump on the sample waiting time.

3.1. Target search

Target search means a protein or protein–DNA/RNA complex locate and bind to a specific sequence on DNA or RNA accurately and efficiently. The distinction of mechanisms resides in the mode of action [27], viz. 1D sliding/hopping, 2D intersegmental transfer, or 3D diffusion. Considering functions of 'target search' in cells, four different kinds of target searches are classified in this review: (i) a protein searching on dsDNA (figure 4(a.1)) [27, 32]; (ii) a protein–ssDNA complex searching on dsDNA (figure 4(b)) [33]; (iii) a protein–RNA complex searching on dsDNA (figure 4(c)) [34, 35]; (iv) and a protein–RNA complex searching on RNA [36, 37].

3.1.1. A protein searches on dsDNA. How a protein searches for its target site on dsDNA is an important question that has been investigated for many years. Multiple theoretical models have been established (figure 4(a.1)) [27, 32] and depicted below. (i) 1D sliding, which means the protein uses thermal energy to diffuse along the length of dsDNA; (ii) 1D hopping, which means the protein moves on dsDNA by a series of microscopic dissociation and rebinding events; (iii) 2D intersegmental transfer, which means the protein can 'jump' between different dsDNA regions by a looped intermediate; (iv) and 3D diffusion, which means the protein will associate with different dsDNA regions directly out of solution, just by diffusion. For non-target regions the binding affinity is low, and only at the target region can the protein bind tightly. Models (i)–(iii) are forms of '*facilitated diffusion*' that can accelerate the search relative to model (iv) 3D diffusion. In the 1970s, Riggs *et al* [38–40] used a nitrocellulose filter binding assay to study the mechanism of target search by the lac repressor. In this assay, the nitrocellulose filter can block the proteins, but not for the dsDNA molecules. dsDNA substrates labeled with radioactivity tags are pre-incubated with the dsDNA binding proteins for various time intervals, and then the total samples are loaded on the filter. Only the free dsDNA substrates can pass through the filter, and the protein-bound dsDNA substrates are retained on the top of the filter. Quantitatively monitoring the temporal change of free dsDNA substrates can provide the target search information. Using this assay, Riggs *et al* proved that the lac repressor locates and binds its target sequence faster than the 3D diffusion limit. In 2006, Wang *et al* [41] used the fluorescence related single-molecule method (section 1) to confirm the same conclusion of the LacI repressor: LacI repressor proteins can perform 1D diffusion along dsDNA. Many researchers have maintained that the cell often entails facilitated diffusion during target search processes.

As an ensemble assay, the nitrocellulose filter binding assay cannot provide direct evidence of facilitated diffusion. In contrast, the dsDNA curtains approach can directly monitor how a single protein moves on dsDNA by analyzing the kymograms (figures 4(a.2) and (a.3)). A kymogram is a particular manipulation and representation of the image stacks, which are the raw data, thus serving as a powerful way to assess the mechanisms of target search. To generate a kymogram, the line images of one DNA substrate from each frame are projected in time and all the frames are plotted together. Then the x-axis corresponds to time, and the y-component represents the sequence of the DNA substrate. The protein is fluorescently labeled, and the signal (in this case represented as magenta lines) shows up on

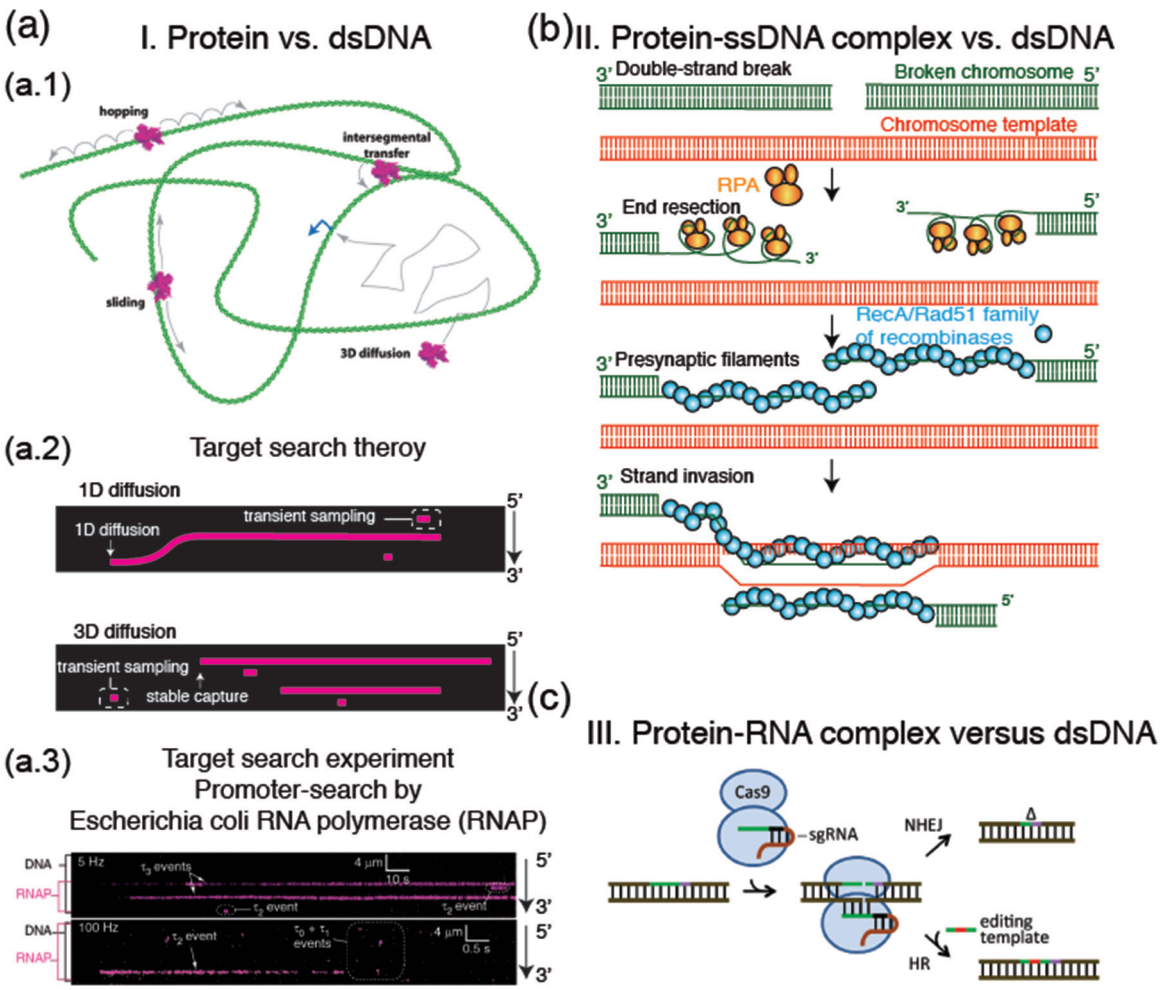

Figure 4. Schematic of a target search. (a) Protein target search on dsDNA. (a.1) Theoretical models for the target search [27]. (a.2) Schematic of dsDNA curtains kymograms for distinguishing different models. (a.3) The real data of kymograms for RNAP searching on dsDNA [27]. (b) A protein–ssDNA complex searching on dsDNA. Figure (b) shows the early stages of HR [43], and homology search [3, 33]; inside is one example for this case. (c) A protein–RNA complex searching on dsDNA. Figure (c) shows a CRISPR-Cas9 system [16, 17], which is a good example for this case. Figures (a.1) and (a.3) are reprinted by permission from Macmillan Publishers Ltd: Nature Structural and Molecular Biology [27], copyright (2012). Figure (b) is reprinted by permission from Macmillan Publishers Ltd: Nature Reviews Molecular Cell Biology [43], copyright (2006). Figure (c) is reprinted from [93], Copyright (2014), with permission from Elsevier.

the kymogram (figure 4(a.2)), revealing how the protein searches for its target. If the fluorescent signals move in the *y*-component (the top figure in figure 4(a.2)), it suggests that the protein undergoes 1D diffusion. However, if the signals are just short straight lines (transient sampling) or long straight lines (stable captures), it suggests the protein is using 3D diffusion to bind DNA (the bottom figure in figure 4(a.2)). In 2013, Wang *et al* [27] used dsDNA curtains method to measure the diffusion coefficients of *Escherichia coli* RNA polymerase (RNAP), and the data is shown in figure 4(a.3), which is a real kymograms. To be surprised, the conclusion is that RNAP performs target search mainly by 3D diffusion. This is the first time to find a target search inside a cell is dominated by 3D diffusion.

Many different protein candidates have been assayed to study the mechanisms of their target search. For example, in eukaryotic replication initiation, the origin recognition complex (ORC) searches for the autonomously replicating sequence 1 (*ARS1*) origin sequence by using both 3D and 1D searching [42]; during DNA mismatch repair, the important protein factor MutSα, which takes charges of recognition of mismatches, also used both 3D and 1D searching mechanisms to find the mismatches [18]. Wang *et al* [27] even found that the concentration of protein determines the fastest target search mechanism: facilitated diffusion matters at low concentrations and 3D diffusion dominates at high concentrations.

3.1.2. Protein–ssDNA complex searches on dsDNA. A typical example of a protein–ssDNA complex searching for a target on dsDNA is the homology search (figure 4(b)) [3, 33] during homologous recombination (HR) mediated DNA break repair. The RecA/Rad51 family of recombinases can form nucleoprotein filaments on ssDNA, which is termed as presynaptic complex (PC) and catalyzes searching on DNA templates to find the complementary region using the ssDNA sequence as a guide [43]. ssDNA curtains approach has been applied to study this problem and the details will be reviews in section 4.4 and figure 10(d).

3.1.3. Protein–RNA complex searches on dsDNA. An important example of a protein–RNA complex searching dsDNA is the CRISPR-Cas9 system, a powerful tool in genome engineering (figure 4(c) and supplementary video 2) [34, 35]. Cas9 is one kind of RNA binding proteins. The Cas9 protein binds a short RNA to form a protein–RNA complex, and the short RNA is complementary to a target sequence. This complex needs to search for the target sequence on dsDNA. It was shown that Cas9–RNA finds targets by 3D diffusion [17], and a similar 3D random collision mechanism has been demonstrated to direct target search by a closely related system [16].

3.1.4. Protein–RNA complex searches on RNA. Examples of protein–RNA complexes that search for targets on RNA are short non-coding RNAs, like small interfering RNA (siRNA) or microRNA [36, 37]. One of the important functions of siRNA/microRNA is: each siRNA/microRNA has a target sequence, and will find the complementary target sequence on messenger RNA. However, RNAs cannot complete these searches independently, and siRNA/microRNA has to bind a protein to form a protein–RNA complex. As this target search involves RNA molecules, the dsDNA curtains method cannot be directly used. Recently other single-molecule methods [44, 45] have been used to explore the mechanism for this kind of target search. However, to better understand this mechanism, we will need to develop a new curtain method for RNA molecules (figure 10(e)). We will discuss this in section 5.

3.2. Protein moving and diffusing on long dsDNA

Some proteins, like helicases/translocases and nucleases, can move on dsDNA on a specific direction ($5' \rightarrow 3'$ or $3' \rightarrow 5'$) with adenosine triphosphate (ATP) hydrolysis. Some other proteins can bind and diffuse on dsDNA without ATP hydrolysis. The dsDNA curtains method can visualize these behaviors. For example, (i) fluorescently labeled heterotrimeric translocase RecBCD displayed rapid movements on dsDNA [15]; (ii) single fluorescent human Rad51 showed the ability to bind and diffuse on dsDNA [46].

3.3. Protein–protein collisions on long dsDNA

Genomic DNA is not naked on both eukaryotes and prokaryotes. It wraps histone proteins to form nucleosomes and then higher order chromatin in eukaryotes, and there are also many different dsDNA binding proteins dynamically coating it. DNA helicases or other motor proteins, for an example, when translocate or unwind a DNA molecule, will likely collide with other protein molecules, such as histones or DNA binding proteins.

The DNA curtains approach has been shown to an effective way for studying protein–protein collisions because long DNA substrates confined to the excitation region of the evanescent wave can be used. Different dsDNA binding proteins can be pre-bound to the DNA molecule to form roadblocks, and the movement of fluorescently labeled motor proteins can be monitored. With these setup, multiple protein–protein collisions on dsDNA have been examined. One great example is the recent study on cohesins [47]. Cohesins are ring shape molecules physically embracing sister-chromatids for their faithful mitotic segregation. As a slider along dsDNA (figure 5(a)), it has been shown that whether cohesins can pass through roadblocks or not depends on the size of roadblocks. Figures 5(b) and (c) show that cohesins can pass through a DIG (~1–2 nm) but fail to pass through a roadblock of DIG + QD (~20 nm). QD means quantum dot, a nanoscale particle (~15–20 nm) made of semiconducting materials. Cohesins can also pass though DNA bound EcoRI^{E111Q} (figures 5(d)), a catalytic null mutant of EcoRI restriction enzyme that binds to DNA, but is unable to cleave it. Cohesins can also pass though single protein dCas9 binding to dsDNA (figure 5(e)). However, it fails again to pass through a roadblock of dCas9 + QD (figure 5(f)). Other examples of protein–protein collisions on dsDNA include: (i) *E. coli* translocase FtsK [48] that can separate chromosome dimers by translocating on dsDNA, where FtsK encounters many roadblock proteins that typically occupy the bacterial chromosome; (ii) *E. coli* RecBCD complex, a helicase-nuclease ensemble that can remove the core RNAP from dsDNA [15]. Although less studied, protein–protein collisions may also occur on RNA, an interesting topic to be discussed in section 5.

3.4. Assembly order

A third application of the dsDNA curtains method is to study assembly order. Initiation of eukaryotic replication [49], as a good example, involves four key components, viz. ORC, Cdc6, Cdt1, and the Mcm2-7 helicase. The function of ORC, Cdc6, and Cdt1 is to recruit Mcm2-7 to origin sequences during a process called pre-replicative complex (pre-RC) formation. By directly monitoring pre-replicative complex assembly on dsDNA curtains, Duzdevich *et al* [42] provided direct evidence on the order of pre-RC assembly. They found that ORC binds dsDNA first, followed by Cdc6 in strict sequence. Together, ORC and Cdc6 recruit Mcm2-7 and Cdt1. The order of binding is tightly regulated and important for the assembly of an active pre-RC.

3.5. Chromatin curtains

Histone protein octamers can be reconstituted on dsDNA substrates to form chromatin curtains. Visnapuu *et al* (supplementary video 3) [50] did this kind of DNA curtains experiments in 2009. The probabilistic nucleosome distributions can be experimentally determined, distinguishing weakly versus strongly bound nucleosome particles. These *in vitro* single-molecule results were compared with three theoretical models for yeast system, Segal *et al* [51], Field *et al* [52], and Kaplan *et al* [53]. To our surprise, the theoretical predictions from Field *et al* [52] and Kaplan *et al* [53] have strong correction with these *in vitro* experimental data. However, Segal *et al* [51] has a strong anti-correction relationship. Field *et al* [52] and Kaplan *et al* [53] can also match some *in vivo* experimental data, but not all [54]. Subsequently, relevant bioinformatic studies on nucleosome positioning on dsDNA have been done, e.g. Teif *et al* [55] and Beshnova *et al* [56]. Chromatin curtains can provide relevant *in vitro* experimental data for these studies, comparing with *in vivo* data.

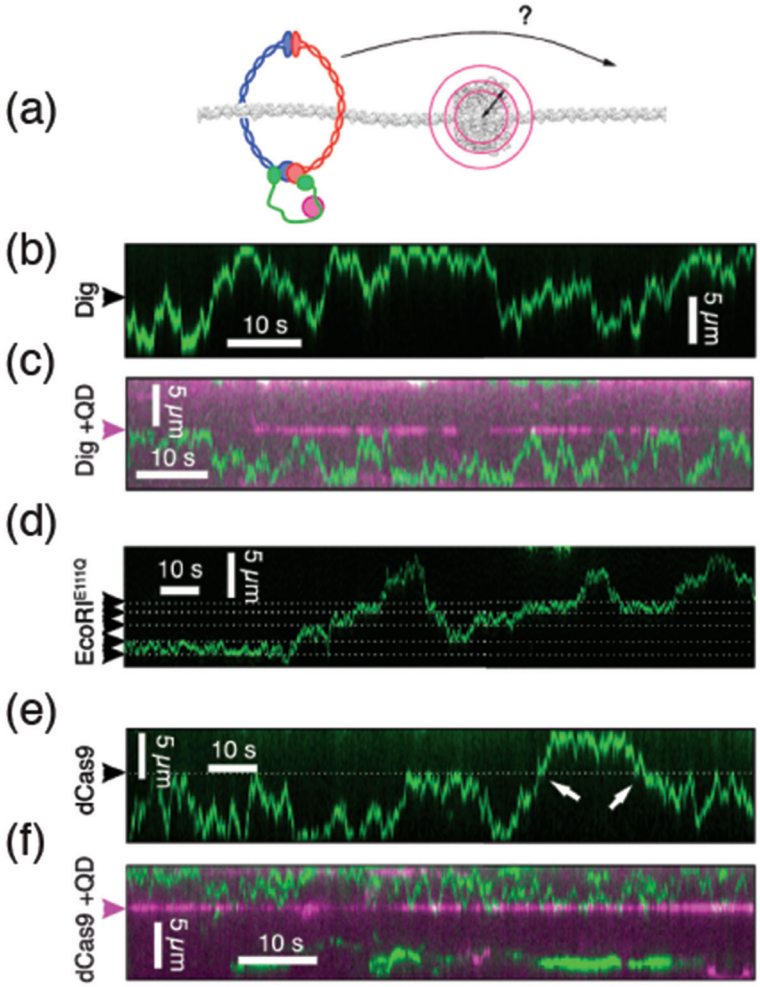

Figure 5. Cohesin-roadblock collisions. (a) Schematic of Cohesin-roadblock collisions. (b) Cohesins pass through DIG. (c) Cohesins cannot pass through DIG-QD. (d) Cohesins pass through $EcoRI^{E111Q}$. (e) Cohesins pass through dCas9. (f) Cohesins cannot pass through dCas9-QD. Reproduced from [47]. CC BY 4.0.

The DNA curtains method is a low-resolution method [12]. EMCCD (Andor Technology, iXon Ultra 897, 512 × 512, 16 μm, 56fps@Full Frame) was applied to detect fluorescent signal. Spatial resolution is 0.27 μm per pixel and temporal resolution is 18-ms. On the monitor window (512 pixels × 512 pixels), one pixel occupies a length of 794 base pairs (bp) dsDNA (1 bp = 0.34 nm for B-form dsDNA), which can reconstitute four nucleosomes (assume a nucleosome octamer takes 147 bp, and the linker region between two nucleosomes is 50 bp). For the current method, Lambda DNA (48 502 bp) is used, occupying 61 pixels. The minimum length of DNA substrate is 5 pixels, which is 3970 bp, and the maximum length is 512 pixels, which is 407 kbp. The nucleosome assembly on dsDNA substrate takes 20 h by a salt dialysis [50]. This step is performed before the DNA curtains experiment. The molar ratio between histone proteins and dsDNA substrate determine dsDNA packing density in the lattice. We can optimize this condition to monitor 1 or 2 nucleosomes per dsDNA substrate, or nucleosomes coating everywhere. Once the nucleosomes bind on DNA, they will be very stable. The DNA curtains experiment can take several hours.

4. Single-stranded DNA curtains

Besides dsDNA, many DNA metabolic processes, such as HR [3], also involve ssDNA as intermediates, which is a research focus in the Greene lab. Indeed, the first biological application on dsDNA curtains [23] was the study of human RAD51 [46], which belongs to the RecA/Rad51 family of recombinases (RecA in bacteria, RadA in archaea, Rad51/Dmc1 in eukaryote, and UvsX in bacteriophages). Compared with dsDNA curtains and other single-molecule methods, a curtains setup with ssDNA substrates, which is called ssDNA curtains, is a better tool for studying HR. ssDNA curtains were firstly developed in 2012 (figure 2) [30]. In contrast to dsDNA, ssDNA has a very short persistence length, and is difficult to be extended by simply a buffer flow. Gibb *et al* [30] confirmed that ssDNA binding protein, replication protein A (RPA), can be used to extend ssDNA into the curtains conformation and simultaneously visualize its structures by the fusion of a green fluorescent protein (GFP) to RPA. Thus, the DNA substrate in ssDNA curtains method are RPA–ssDNA complexes, coincidently mimicking the biological conditions in cells, where the crucial initial step of genome maintenance processes [57–59]

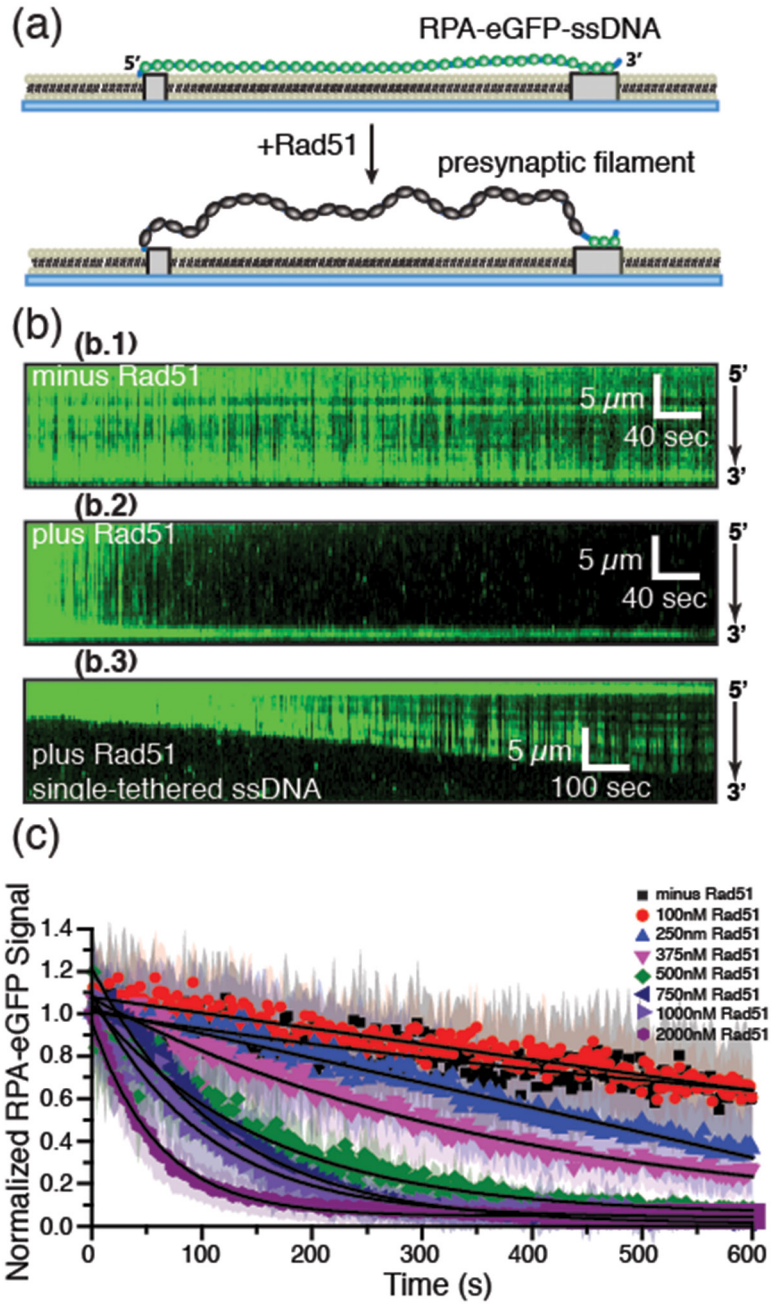

Figure 6. PC formation. (a) Schematic of scRad51 exchanging scRPA–eGFP on ssDNA. (b) Kymograms of raw data: (b.1) DT molecule without scRad51; (b.2) DT molecule with scRad51; (b.3) single-tethered molecule with scRad51. (c) The scRad51 concentration affects the exchange rate. Reproduced from [73]. CC BY 4.0.

like DNA replication, repair, and recombination, is always separating the double-stranded genomic DNA into its component ssDNA [60]. Once the nascent ssDNA [61] appears, SSB (the name in prokaryotes) or RPA (the name in eukaryotes) monomers are generally the first to bind the ssDNA and, among other functions [61, 62], safeguard the ssDNA from degradation, reduce its secondary structure, regulate helicase unwinding activity [63, 64], and recruit repair enzymes to DNA damage sites [65, 66]. The second step usually involves exchanging RPA/SSB with other proteins, like RecA/Rad51 recombinases during HR [43].

The ssDNA curtains method has been successfully applied to study the early stages of HR (figure 4(c)) [12, 67, 68]. Both eukaryotes and prokaryotes have the DNA genome that can be damaged by genotoxic agents in the environment, e.g. carcinogenic chemicals or ionizing radiation, or even by natural cellular process [69]. Double-stranded DNA breaks (DSBs) are among the most toxic DNA lesions (figure 4(c)) because they can lead to chromosomal rearrangements, a hallmark of all forms of cancer [70]. Fortunately, rather than simply succumbing to this onslaught of damage, the cells have the ability to repair broken chromosomes. HR [43] is an important error-free pathway that allows the cells to use sequence information encoded by the homologous chromosome as a template to guide the repair of broken chromosomes. However, for this to occur, members of the RecA/Rad51 family of recombinases

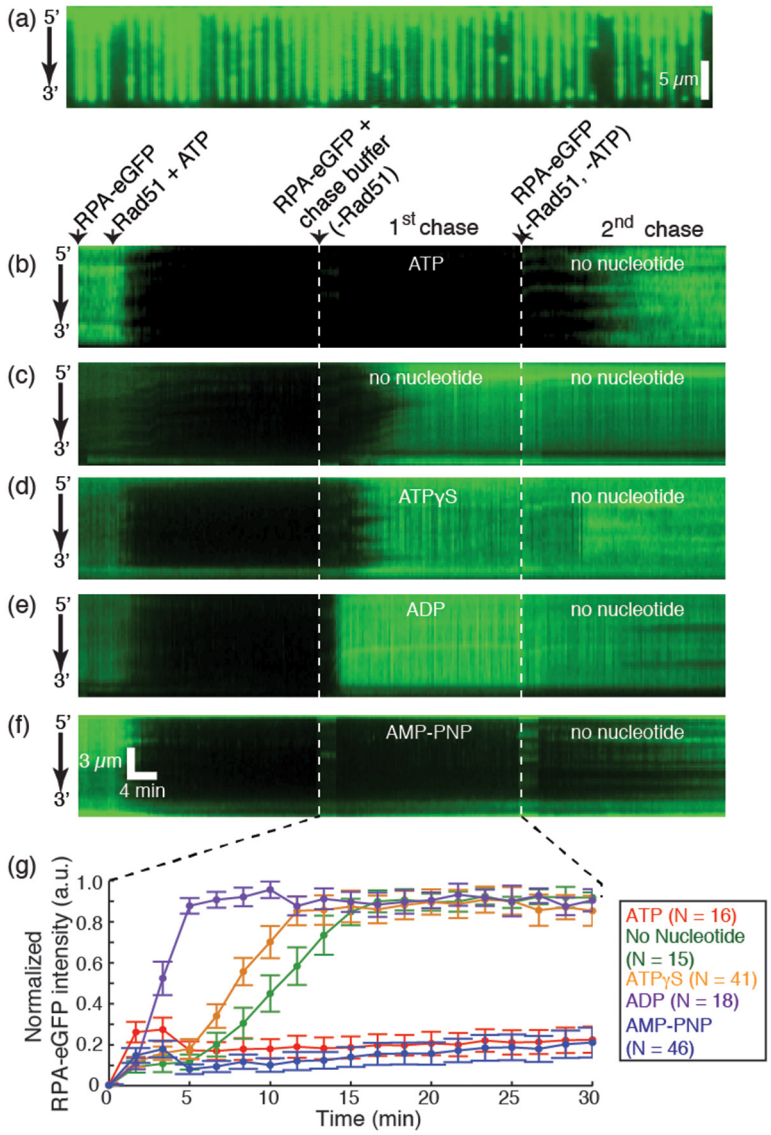

Figure 7. PC stability. (a) Wide-field TIRFM image of the RPA–eGFP–ssDNA complex. (b)–(f) Kymograms of PCs under different buffer conditions (1st chase): (b) ATP; (c) no nucleotide; (d) ATPγS; (e) ADP; (f) AMP-PNP. (g) The RPA–eGFP signals versus time during the 1st chase. Reprinted from [73], Copyright (2015), with permission from Elsevier.

must first exchange RPA to form PCs (sections 4.1–4.3) and search through vast amounts of DNA to align the broken chromosome ends with the undamaged template (section 4.4).

4.1. PC formation

ssDNA curtains have been used to visualize how Rad51/RecA exchanges RPA and assembles PCs (figure 6) [3, 30, 71]. ssDNA substrates are extended to form an RPA–ssDNA complex in the presence of RPA–eGFP (figure 2) [3, 30, 71]. *Saccharomyces cerevisiae* Rad51 (scRad51) at different concentrations is injected into the flowcell to exchange RPA–eGFP, forming PCs (figure 6(a)) [3, 30, 71]. The exchange rate can be measured from the kymograms (figures 6(b) and (c)). Figure 6(b.2) shows that the eGFP intensity rapidly decays due to the exchange of previously bound RPA–eGFP with the unlabeled scRad51 molecules. In the absence of scRad51, the RPA–eGFP signal remains constant (figure 6(b.1)). The titration experiments in figure 6(c) demonstrate that the exchange rate depends on the scRad51 concentration, suggesting an assembly mechanism for scRad51 that can be studied in the future. PC formation extends the average nucleotide–nucleotide distance of ssDNA [72, 73], causing the DNA substrate to extend. The single-tethered experiment in figure 6(b.3) demonstrates this stretching effect. Since both ends are fixed in the case of a DT molecule, this stretching effect causes ssDNA molecules to become 'floppy' (figure 6(a)).

4.2. PC Stability

To study downstream reactions of HR, a crucial question has to be answered: 'How long can PCs remain stable *in vitro*?' Following the PC assembling, an interesting question is to examine the stability of PCs. To test this, a set of ssDNA curtain experiments was designed to test PC stability *in vitro*

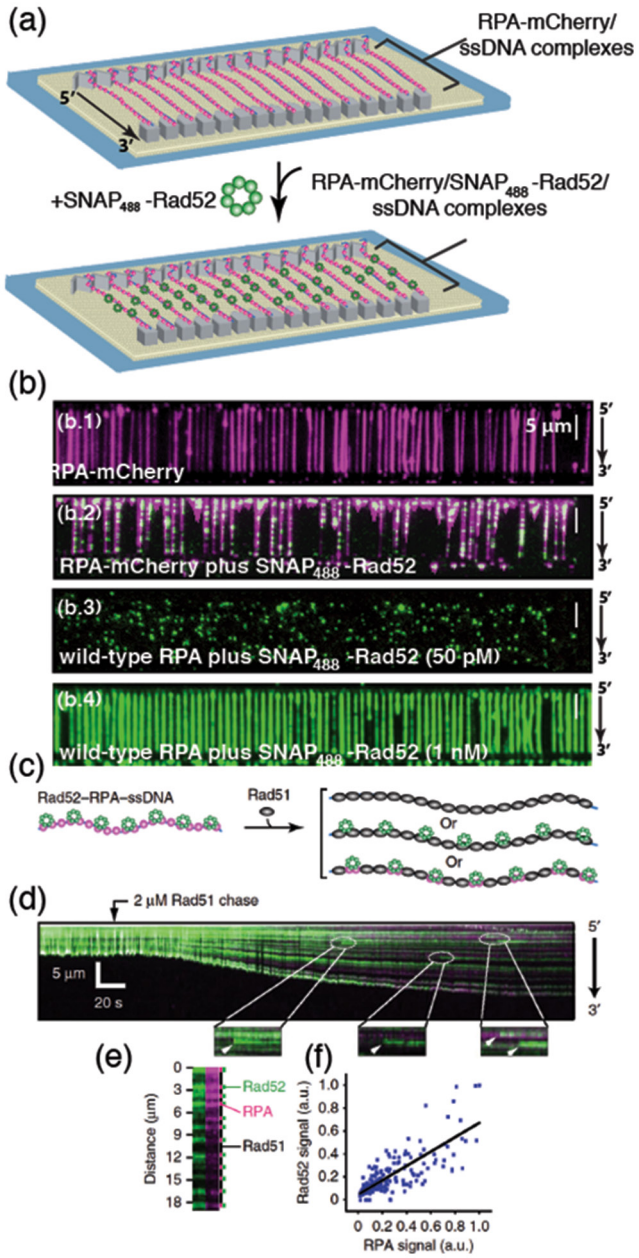

Figure 8. Protein dynamics on PCs. (a) Schematic of scRad52-$SNAP_{488}$ complex (green color) binding on RPA-mCherry (red color). (b) Wide-filed images of scRPA curtains with scRad52 under different conditions: (b.1) scRPA-mCherry curtains without Rad52; (b.2) scRPA-mCherry curtains with 50 pM scRad52-$SNAP_{488}$; (b.3) WT scRPA curtains with 50 pM scRad52-$SNAP_{488}$; (iv) WT scRPA curtains with 1 nM scRad52-$SNAP_{488}$. (c) Schematic of three models of the scRad52 and scRPA dynamics on PC assembly. (d) A representative single-tethered kymogram. (e) and (f) Data analysis to confirm the colocalization of scRad52 with scRPA. Reprinted by permission from Macmillan Publishers Ltd: Nature Structural and Molecular Biology [76], copyright (2014).

(figure 7) [3]. After the formation of stable RPA–ssDNA complexes (figure 7(a)), scRad51 and ATP are injected into the flowcell, assembling active PCs. Afterwards, different buffers, including buffer containing 1 nM RPA–eGFP (same as the starting condition), 30 mM Tris-Acetate (pH 7.5), 20 mM Mg-Acetate, 50 mM KCl, 1 mM DTT, 0.2 mg ml^{-1} BSA in the absence or presence ATP, or its analogues (2.5 mM ATP in figure 7(b); no ATP in figure 7(c); 2.5 mM ATPγS in figure 7(d); 2.5 mM ADP in figure 7(e); 2.5 mM AMP-PNP in figure 7(f)) are loaded into the flowcell. All these buffers are free of scRad51 to monitor binding of RPA–eGFP upon scRad51 turnover from ssDNA. The eGFP intensity plotted against time for each case is shown in figure 7(g). The results showed that PC remains stable in presence of ATP or AMP-PNP, but not stable in the presence of ADP or ATPγS, in the absence of nucleotides.

4.3. Protein dynamics on PCs

ssDNA curtains provide a good experimental setup to directly monitor protein dynamics on the PCs. Gibb *et al* [74] recently investigated how *S. cerevisiae* RPA (scRPA) and *S. cerevisiae* Rad52 (scRad52) complexes, a mediator protein that interacts with both scRad51 and RPA and promotes scRad51 PC formation (figure 8). Once stable RPA–ssDNA complexes are formed on DT curtains (figures 8(a) and (b.1), scRad52 complexes are injected into the flowcell (figures 8(a) and (b)), and scRad52 complexes can interact with ssDNA or ssDNA-bound RPA molecules. To confirm the binding mode of scRad52 complexes, the same experiment is also repeated on single-tethered curtains (figures 8(c) and (d)). In this experiment, after scRad52 complexes bind to RPA–ssDNA curtains, wild type scRad51 molecules with ATP are injected into this single-tethered curtains. Three possible models are depicted in figure 8(c): (i) scRad51 forms a PC by displacing all scRPA and scRad52 on ssDNA; (ii) scRad51 forms a PC by displacing all scRPA monomers on ssDNA; (iii) scRad51 forms a PC by only displacing the scRPA monomers that do not bind with scRad52 complexes. The result is shown in figure 8(d). The analysis in figures 8(e) and (f) shows that the third model is correct. The green color signal and red color signal co-localize together, confirming that scRad52 complexes (green color) bound to the local RPA molecules (red color) remains on the single-tethered curtains.

4.4. Homology search mechanism

In a recent study, Qi *et al* [3] used ssDNA-curtains (figure 9) to visualize scRad51-catalzyed alignment and pairing with homologous DNA sequences in real-time. When active scRad51 PCs are formed (figure 9(a)), 70 bp dsDNA with different lengths of microhomology are injected into the flowcell (figure 9(b)). After a short (~10 min) incubation, the flow is turned on to wash out all free dsDNA (figure 9(b)). Then the data acquisition is started to monitor how PCs interrogate the dsDNA with different lengths of microhomology (figure 9(c) and supplementary video 5). The dsDNA is labeled with a fluorescent dyes (Atto565). A typical kymograph showing dsDNA dissociation is in figure 9(d). The results demonstrated that microhomology sampling is the key point to direct homology search: (i) during interrogating dsDNA, RecA/Rad51 family members enable robust kinetic selection of 8-nucleotide tracts of microhomology, which kinetically confines the search to sites with a high probability of being a homologous target;

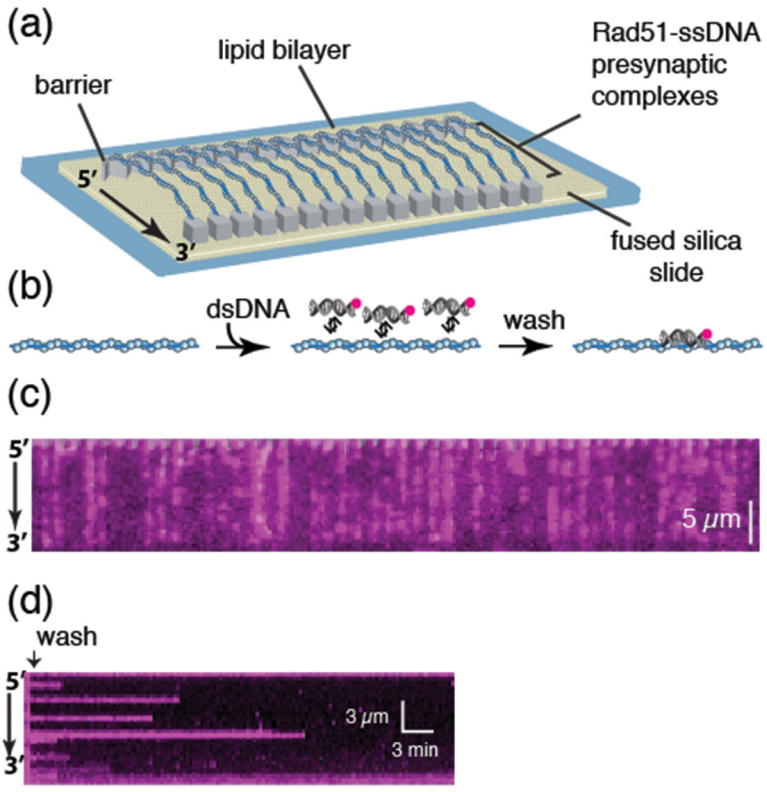

Figure 9. Homology search mechanism [3]. (a) Schematic of scRad51 PC assembly. (b) Schematic of the first method. (c) Wide-field image of PCs bound to 70 bp dsDNA with a fluorescent dyes (Atto565). (d) A representative kymograph showing dsDNA dissociation. Reprinted from [3], Copyright (2015), with permission from Elsevier.

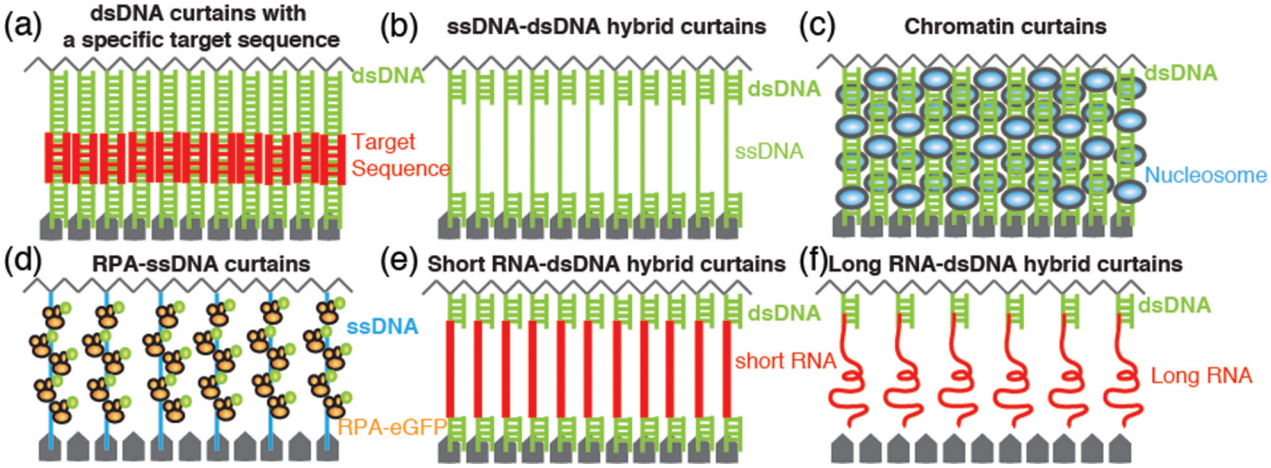

Figure 10. Schematic of curtains. (a) dsDNA curtains with a specific target sequence; (b) ssDNA–dsDNA hybrid curtains; (c) chromatin curtains [50]; (d) RPA–ssDNA curtains [30]; (e) short RNA–dsDNA curtains; (f) long RNA–dsDNA curtains.

(ii) RecA/Rad51 family members rapidly sample and reject dsDNA with less than 8-nucleotide tracts of microhomology through a mechanism characterized by its distinctive power-law dependence; (iii) successful pairing with a 9th nucleotide coincides with an additional reduction in binding free energy and subsequent strand exchange occurs in precise 3-nucleotide steps, reflecting the base triplet organization of the PC. This conclusion is also shown in [2] (iv) dsDNA binding on the PC by a short length of microhomology can be disrupted by other dsDNA molecules with an equal or longer microhomology length. This process is termed facilitated exchange, and it depends on the microhomology length and sequence. These findings provide crucial new insights into the physical and evolutionary underpinnings of DNA recombination.

5. Conclusions and future directions

By removing ensemble averaging, single-molecule techniques can explore heterogeneity across molecules and reactions, and monitor transient intermediate states in real-time [75]. The dsDNA and ssDNA curtains approaches have powerful tools in single-molecule biophysics for studying protein–DNA

interactions. We have reviewed the past and present of the DNA curtains method, including development of nanofabrication techniques for the high-throughput analysis of reactions involving individual DNA molecules, the applications of dsDNA curtains method to study the target search, protein movement, diffusion, and protein–protein collisions on long dsDNA, and the order of reaction center assembly, and how the applications of the ssDNA curtains method has been used to study PCs during HR.

Besides the Greene lab, another two labs are doing dsDNA curtains experiments: (i) the O'Donnell lab (Rockefeller University). They applied dsDNA curtains to monitor *E. coli* replisomes in real-time [76, 77]. The replisome is a team of proteins that takes charge of DNA replication; (ii) the Finkelstein lab (University of Texas at Austin): (1) protein moving on long dsDNA (section 3.2). They studied how Exonuclease 1 (Exo1) moved and digested on dsDNA [78]. (2) Protein–protein collisions on long dsDNA (section 3.3). They studied how DNA repair factor MutSα bypassed different roadblocks, like EcoRI mutant E111Q and nucleosomes [79].

As a new single-molecule method, DNA curtains has a bright future. Here we discuss three short-term future directions and one long-term future direction. The first short-term future direction is to develop new DNA/RNA substrates to delineate many other biological reactions that demand single-molecule approach to reveal their molecular underpinnings (figure 10):

(i) dsDNA curtains with a specific target sequence (figure 10(a)). The short specific target sequence can be cloned into the dsDNA molecule. This substrate can be used to study the specificity of protein–DNA interactions [80], especially the transcription factors (TFs) binding on its target sequence, which is called 'response elements' (REs) [81]. How to search and bind on correct REs by TFs is a crucial cell process for transcription. Many high-throughput experimental methods [80], e.g. the mechanically induced trapping of molecular interactions (MITOMI) and surface plasmon resonance (SPR), are developed to determine REs by measuring the binding constants of TFs on dsDNA. However, these ensemble methods can not directly observe how TFs finds REs, which maybe includes: (1) TFs binding on non-specific sites; (2) TFs sliding on dsDNA; (3) TFs finding and tightly binding on REs; (4) TFs dissociating from REs and keeping slide on dsDNA or completely dissociating from dsDNA. To monitor all these short intermediate states, single-molecule techniques, especially dsDNA curtains with a specific RE is a better method. However, no dsDNA curtains experiments have been published until now, suggesting the difficulties. One of the most difficult points is that the normal TFs are not stable *in vitro*, increasing the hardness of protein expression and purification. Monitoring the recognition of REs by TFs *in vitro* is not easy for some unknown reasons. For example, another fluorescence related single-molecule method was applied to study the tumor suppressor p53 [82]. Only p53 diffusion on dsDNA were monitored, and little evidence to display p53 can find and stop on its RE. We really hope dsDNA curtains with different REs can be used to successfully observe the recognition of REs by TFs, measuring the binding constants of TFs on REs and non-REs, and also the diffusion coefficient of TFs on dsDNA.

(ii) ssDNA–dsDNA hybrid curtains (figure 10(b)) could be used to study proteins that bind dsDNA and ssDNA at the same time, like the RecA/Rad51 family of recombinases.

(iii) Chromatin curtains (section 3.5 and figure 10(c)). Chromatin curtains [50] can be used to study nucleosome–protein interactions, which are of greater biological relevance than naked DNA substrates.

(iv) Short RNA–dsDNA hybrid curtains (figure 10(e)). These substrates can be used to study siRNA/microRNA searching for targets on messenger RNA (section 3.1.4).

(v) Long RNA–dsDNA hybrid curtains (figure 10(f)) could be used to study protein–protein collisions on RNA.

(vi) Protein curtains. DNA substrates can be exchanged with proteins. Actin is one of the most important cytoskeletal proteins, forming actin filaments. Actin filaments inside living cells can also form bundles or 3D networks, providing mechanical support for cell shape and surface. Lieleg *et al* [83] applied the confocal microscopy to directly observe the formation of cytoskeleton networks of actin filaments *in vitro*. To apply the curtains method, Courtemanche *et al* [84] used actin filaments as the substrates to form actin filament curtains and studied actin monomer assembly. However, actin filament curtains is an *in vitro* method now, and we cannot directly apply this detection method inside living cells, which is our long-term future direction.

The second short-term direction is to update the flowcell preparation: (i) testing other nanofabrication methods for diffusion barrier preparation. Electron-beam lithography can provide the best resolution with 100 nm barrier width. However, the procedure is complicated and expensive. Recently, the Finkelstein lab showed that UV lithography could replace of electron-beam lithography to generate diffusion barriers [85]. UV lithography is easier to use, however, it sacrifices resolution. The barrier width increases to more than 1000–2000 nm. Further work is needed to improve this method to get the barrier width closer to 100 nm; (ii) producing a multichannel flowcell. The Finkelstein lab developed a new multichannel flowcell [86], to allow ATP titration experiments can be performed in a single flowcell experiment.

The third short-term direction is to mimic the internal macromolecular crowding of living cells [87]. The DNA curtains method is an *in vitro* assay, and the normal working buffer prepared for the single-molecule experiments is too simple to mimic the realistic conditions inside living cells. A living cell can be assumed as a molecule factory in which the space inside is highly crowded. To mimic the internal macromolecular crowding, two methods are used: (i) adding biological elements of living cells into the working buffer gradually. The advantage of this method is the working buffer condition is explicit. However, it will take long time to reach the final living cell condition because there are still many unknown elements, e.g. proteins; (ii) adding a cell extract. Cell lysis

is applied to damage and remove cell membrane, and the free solution inside is the cell extract that remain the most elements. The cell extract can be used as a working buffer, mimicking the realistic conditions inside living cells. This method has been developed, e.g. (1) *Xenopus laevis* cell-free extracts are applied to research DNA replication [88]; (2) whole-cell extracts are used for single spliceosomes assembly [89]. The benefit of this method is pushing *in vitro* single-molecule biophysics towards physiological complexity faster [31]. However, the unknown elements inside the cell extract are still the difficulty, which needs to be faced with.

Some single-molecule techniques have been developed to monitor protein–DNA interactions at realistic conditions inside living cells [90–92]. However, DNA curtains is still an *in vitro* method now. As a longer-term goal, we hope to leverage DNA curtains to develop systems that will allow researchers to address the physical nature of these crucial biological reactions, as well as gain an understanding of precisely how they occur inside of living cells.

Acknowledgments

We thank Dr Hengyao Niu (Indiana University, USA) for comments and edits on our manuscript. The composition of this review was funded by a start-up fund from the Center for Quantitative Biology and Peking-Tsinghua Center for Life Sciences at Peking University (China) and the NSF of China (Grant No. 31670762).

References

[1] Alberts B *et al* 2008 *Molecular Biology of the Cell* 5th edn (New York: Garland)
[2] Lee J Y *et al* 2015 DNA recombination. Base triplet stepping by the Rad51/RecA family of recombinases *Science* **349** 977–81
[3] Qi Z *et al* 2015 DNA sequence alignment by microhomology sampling during homologous recombination *Cell* **160** 856–69
[4] Joo C *et al* 2006 Real-time observation of RecA filament dynamics with single monomer resolution *Cell* **126** 515–27
[5] Bell J C *et al* 2012 Direct imaging of RecA nucleation and growth on single molecules of SSB-coated ssDNA *Nature* **491** 274-U144
[6] Forget A L and Kowalczykowski S C 2012 Single-molecule imaging of DNA pairing by RecA reveals a three-dimensional homology search *Nature* **482** 423–7
[7] Ragunathan K, Joo C and Ha T 2011 Real-time observation of strand exchange reaction with high spatiotemporal resolution *Structure* **19** 1064–73
[8] Ragunathan K, Liu C and Ha T 2012 RecA filament sliding on DNA facilitates homology search *eLife* **1** e00067
[9] Selvin P R and Ha T 2008 *Single Molecule Techniques: A Laboratory Manual* (New York: Cold Spring Harbor Laboratory Press) p 37
[10] Roy R, Hohng S and Ha T 2008 A practical guide to single-molecule FRET *Nat. Methods* **5** 507–16
[11] Greene E C *et al* 2010 DNA curtains for high-throughput single-molecule optical imaging *Single Molecule Tools, Pt A: Fluorescence Based Approaches* (*Methods in Enzymology* vol 472) ed N G Walter (San Diego, CA: Elsevier) pp 293–315
[12] Qi Z and Greene E C 2016 Visualizing recombination intermediates with single-stranded DNA curtains *Methods* **105** 62–74
[13] Neuman K C and Nagy A 2008 Single-molecule force spectroscopy: optical tweezers, magnetic tweezers and atomic force microscopy *Nat. Methods* **5** 491–505
[14] Jain A *et al* 2011 Probing cellular protein complexes using single-molecule pull-down *Nature* **473** 484-U322
[15] Finkelstein I J, Visnapuu M L and Greene E C 2010 Single-molecule imaging reveals mechanisms of protein disruption by a DNA translocase *Nature* **468** 983–7
[16] Redding S *et al* 2015 Surveillance and processing of foreign DNA by the *Escherichia coli* CRISPR-cas system *Cell* **163** 854–65
[17] Sternberg S H *et al* 2014 DNA interrogation by the CRISPR RNA-guided endonuclease Cas9 *Nature* **507** 62–7
[18] Gorman J *et al* 2012 Single-molecule imaging reveals target-search mechanisms during DNA mismatch repair *Proc. Natl Acad. Sci. USA* **109** E3074–83
[19] Finkelstein I J and Greene E C 2013 Molecular traffic jams on DNA *Annu. Rev. Biophys.* **42** 241–63
[20] Duzdevich D, Redding S and Greene E C 2014 DNA dynamics and single-molecule biology *Chem. Rev.* **114** 3072–86
[21] Silverstein T D, Gibb B and Greene E C 2014 Visualizing protein movement on DNA at the single-molecule level using DNA curtains *DNA Repair* **20** 94–109
[22] Finkelstein I J and Greene E C 2011 Supported lipid bilayers and DNA curtains for high-throughput single-molecule studies *Methods Mol. Biol.* **745** 447–61
[23] Graneli A *et al* 2006 Organized arrays of individual DNA molecules tethered to supported lipid bilayers *Langmuir* **22** 292–9
[24] Visnapuu M L, Duzdevich D and Greene E C 2008 The importance of surfaces in single-molecule bioscience *Mol. Biosyst.* **4** 394–403
[25] Visnapuu M L *et al* 2008 Parallel arrays of geometric nanowells for assembling curtains of DNA with controlled lateral dispersion *Langmuir* **24** 11293–9
[26] Fazio T *et al* 2008 DNA curtains and nanoscale curtain rods: high-throughput tools for single molecule imaging *Langmuir* **24** 10524–31
[27] Wang F *et al* 2013 The promoter-search mechanism of *Escherichia coli* RNA polymerase is dominated by three-dimensional diffusion *Nat. Struct. Mol. Biol.* **20** 174–81
[28] Gorman J *et al* 2010 Nanofabricated racks of aligned and anchored DNA substrates for single-molecule imaging *Langmuir* **26** 1372–9
[29] Gorman J *et al* 2007 Dynamic basis for one-dimensional DNA scanning by the mismatch repair complex Msh2-Msh6 *Mol. Cell* **28** 359–70
[30] Gibb B *et al* 2012 Single-stranded DNA curtains for real-time single-molecule visualization of protein–nucleic acid interactions *Anal. Chem.* **84** 7607–12
[31] Duzdevich D and Greene E C 2013 Towards physiological complexity with *in vitro* single-molecule biophysics *Phil. Trans. R. Soc.* B **368** 20120271
[32] Gorman J and Greene E C 2008 Visualizing one-dimensional diffusion of proteins along DNA *Nat. Struct. Mol. Biol.* **15** 768–74
[33] Renkawitz J, Lademann C A and Jentsch S 2014 DNA damage mechanisms and principles of homology search during recombination *Nat. Rev. Mol. Cell Biol.* **15** 369–83
[34] Lander E S 2016 The heroes of CRISPR *Cell* **164** 18–28
[35] Wright A V, Nunez J K and Doudna J A 2016 Biology and applications of CRISPR systems: harnessing nature's toolbox for genome engineering *Cell* **164** 29–44

[36] Bartel D P 2009 MicroRNAs: target recognition and regulatory functions *Cell* **136** 215–33
[37] Gorman C and Maron D F 2014 The RNA revolution *Sci. Am.* **310** 52–9
[38] Riggs A D, Bourgeois S and Cohn M 1970 The lac repressor–operator interaction. 3. Kinetic studies *J. Mol. Biol.* **53** 401–17
[39] Riggs A D, Newby R F and Bourgeois S 1970 Lac repressor–operator interaction. II. Effect of galactosides and other ligands *J. Mol. Biol.* **51** 303–14
[40] Riggs A D, Suzuki H and Bourgeois S 1970 Lac repressor–operator interaction. I. Equilibrium studies *J. Mol. Biol.* **48** 67–83
[41] Wang Y M, Austin R H and Cox E C 2006 Single molecule measurements of repressor protein 1D diffusion on DNA *Phys. Rev. Lett.* **97** 048302
[42] Duzdevich D *et al* 2015 The dynamics of eukaryotic replication initiation: origin specificity, licensing, and firing at the single-molecule level *Mol. Cell* **58** 483–94
[43] Sung P and Klein H 2006 Mechanism of homologous recombination: mediators and helicases take on regulatory functions *Nat. Rev. Mol. Cell Biol.* **7** 739–50
[44] Chandradoss S D *et al* 2015 A dynamic search process underlies MicroRNA targeting *Cell* **162** 96–107
[45] Salomon W E *et al* 2015 Single-molecule imaging reveals that argonaute reshapes the binding properties of its nucleic acid guides *Cell* **162** 84–95
[46] Graneli A *et al* 2006 Long-distance lateral diffusion of human Rad51 on double-stranded DNA *Proc. Natl Acad. Sci. USA* **103** 1221–6
[47] Stigler J *et al* 2016 Single-molecule imaging reveals a collapsed conformational state for DNA-bound cohesin *Cell Rep.* **15** 988–98
[48] Lee J Y *et al* 2014 Single-molecule imaging of FtsK translocation reveals mechanistic features of protein–protein collisions on DNA *Mol. Cell* **54** 832–43
[49] Mechali M 2010 Eukaryotic DNA replication origins: many choices for appropriate answers *Nat. Rev. Mol. Cell Biol.* **11** 728–38
[50] Visnapuu M L and Greene E C 2009 Single-molecule imaging of DNA curtains reveals intrinsic energy landscapes for nucleosome deposition *Nat. Struct. Mol. Biol.* **16** 1056–62
[51] Segal E *et al* 2006 A genomic code for nucleosome positioning *Nature* **442** 772–8
[52] Field Y *et al* 2008 Distinct modes of regulation by chromatin encoded through nucleosome positioning signals *Plos Comput. Biol.* **4** 25
[53] Kaplan N *et al* 2009 The DNA-encoded nucleosome organization of a eukaryotic genome *Nature* **458** 362–6
[54] Mavrich T N *et al* 2008 A barrier nucleosome model for statistical positioning of nucleosomes throughout the yeast genome *Genome Res.* **18** 1073–83
[55] Teif V B *et al* 2012 Genome-wide nucleosome positioning during embryonic stem cell development *Nat. Struct. Mol. Biol.* **19** 1185
[56] Beshnova D A *et al* 2014 Regulation of the Nucleosome repeat length *in vivo* by the DNA sequence, protein concentrations and long-range interactions *Plos Comput. Biol.* **10** 14
[57] Richard D J *et al* 2008 Single-stranded DNA-binding protein hSSB1 is critical for genomic stability *Nature* **453** 677–81
[58] Kowalczykowski S C *et al* 1994 Biochemistry of homologous recombination in *Escherichia coli Microbiol. Rev.* **58** 401–65
[59] Kuzminov A 1999 Recombinational repair of DNA damage in *Escherichia coli* and bacteriophage lambda *Microbiol. Mol. Biol. Rev.* **63** 751–813
[60] Ha T, Kozlov A G and Lohman T M 2012 Single-molecule views of protein movement on single-stranded DNA *Annual Review of Biophysics* vol 41, ed D C Rees (Palo Alto: Annual Reviews) pp 295–319
[61] Shereda R D *et al* 2008 SSB as an organizer/mobilizer of genome maintenance complexes *Crit. Rev. Biochem. Mol. Biol.* **43** 289–318
[62] Wold M S 1997 Replication protein A: a heterotrimeric, single-stranded DNA-binding protein required for eukaryotic DNA metabolism *Annu. Rev. Biochem.* **66** 61–92
[63] Harmon F G and Kowalczykowski S C 2001 Biochemical characterization of the DNA helicase activity of the *Escherichia coli* RecQ helicase *J. Biol. Chem.* **276** 232–43
[64] Rajagopal V and Patel S S 2008 Single strand binding proteins increase the processivity of DNA unwinding by the hepatitis C virus helicase *J. Mol. Biol.* **376** 69–79
[65] Cubeddu L and White M F 2005 DNA damage detection by an archaeal single-stranded DNA-binding protein *J. Mol. Biol.* **353** 507–16
[66] Woodman I L, Brammer K and Bolt E L 2011 Physical interaction between archaeal DNA repair helicase Hel308 and replication protein A (RPA) *DNA Repair* **10** 306–13
[67] Greene E C 2016 On the influence of protein–DNA register during homologous recombination *Cell Cycle* **15** 172–5
[68] Greene E C 2016 DNA sequence alignment during homologous recombination *J. Biol. Chem.* **291** 11572–80
[69] De Bont R and van Larebeke N 2004 Endogenous DNA damage in humans: a review of quantitative data *Mutagenesis* **19** 169–85
[70] Helleday T *et al* 2008 DNA repair pathways as targets for cancer therapy *Nat. Rev. Cancer* **8** 193–204
[71] Gibb B *et al* 2014 Concentration-dependent exchange of replication protein A on single-stranded DNA revealed by single-molecule imaging *PLoS One* **9** e87922
[72] Chen Z C, Yang H J and Pavletich N P 2008 Mechanism of homologous recombination from the RecA-ssDNA/dsDNA structures *Nature* **453** 489–94
[73] Kowalczykowski S C 2008 Structural biology—snapshots of DNA repair *Nature* **453** 463
[74] Gibb B *et al* 2014 Protein dynamics during presynaptic-complex assembly on individual single-stranded DNA molecules *Nat. Struct. Mol. Biol.* **21** 893–900
[75] Michalet X *et al* 2007 Detectors for single-molecule fluorescence imaging and spectroscopy *J. Mod. Opt.* **54** 239
[76] Georgescu R E, Kurth I and O'Donnell M E 2012 Single-molecule studies reveal the function of a third polymerase in the replisome *Nat. Struct. Mol. Biol.* **19** 113–6
[77] Yao N Y *et al* 2009 Single-molecule analysis reveals that the lagging strand increases replisome processivity but slows replication fork progression *Proc. Natl Acad. Sci. USA* **106** 13236–41
[78] Myler L R *et al* 2016 Single-molecule imaging reveals the mechanism of Exo1 regulation by single-stranded DNA binding proteins *Proc. Natl Acad. Sci. USA* **113** E1170–9
[79] Brown M W *et al* 2016 Dynamic DNA binding licenses a repair factor to bypass roadblocks in search of DNA lesions *Nat. Commun.* **7** 10607
[80] Stormo G D and Zhao Y 2010 Determining the specificity of protein–DNA interactions *Nat. Rev. Genet.* **11** 751–60
[81] Pan Y P *et al* 2010 Mechanisms of transcription factor selectivity *Trends Genet.* **26** 75–83
[82] Tafvizi A *et al* 2011 A single-molecule characterization of p53 search on DNA *Proc. Natl Acad. Sci. USA* **108** 563–8
[83] Lieleg O *et al* 2011 Slow dynamics and internal stress relaxation in bundled cytoskeletal networks *Nat. Mater.* **10** 236–42
[84] Courtemanche N *et al* 2013 Tension modulates actin filament polymerization mediated by formin and profilin *Proc. Natl Acad. Sci. USA* **110** 9752–7

[85] Gallardo I F *et al* 2015 High-throughput universal DNA curtain arrays for single-molecule fluorescence imaging *Langmuir* **31** 10310–7
[86] Robison A D and Finkelstein I J 2014 Rapid prototyping of multichannel microfluidic devices for single-molecule DNA curtain imaging *Anal. Chem.* **86** 4157–63
[87] McGuffee S R and Elcock A H 2010 Diffusion, crowding & protein stability in a dynamic molecular model of the bacterial cytoplasm *Plos Comput. Biol.* **6** 18
[88] Yardimci H *et al* 2012 Single-molecule analysis of DNA replication in Xenopus egg extracts *Methods* **57** 179–86
[89] Hoskins A A *et al* 2011 Ordered and dynamic assembly of single spliceosomes *Science* **331** 1289–95
[90] Doksani Y *et al* 2013 Super-resolution fluorescence imaging of telomeres reveals TRF2-dependent T-loop formation *Cell* **155** 345–56
[91] Zhao Z Q W *et al* 2014 Spatial organization of RNA polymerase II inside a mammalian cell nucleus revealed by reflected light-sheet superresolution microscopy *Proc. Natl Acad. Sci. USA* **111** 681–6
[92] Xie X S *et al* 2008 Single-molecule approach to molecular biology in living bacterial cells *Annual Review of Biophysics* (Palo Alto: Annual Reviews) pp 417–44
[93] Barrangou R and Marraffini L A 2014 CRISPR-Cas systems: prokaryotes upgrade to adaptive immunity *Mol. Cell* **54** 234–44